

Structure of the unbound ^{11}N nucleus by the ($^3\text{He}, ^6\text{He}$) reaction

V. Guimarães,¹ S. Kubono,² F. C. Barker,³ M. Hosaka,⁴ S. C. Jeong,⁵ I. Katayama,⁵ T. Miyachi,² T. Nomura,⁵ M. H. Tanaka,⁵ Y. Fuchi,⁵ H. Kawashima,⁵ S. Kato,⁶ C. C. Yun,⁷ K. Ito,⁷ H. Orihara,⁷ T. Terakawa,⁷ T. Kishida,⁸ Y. Pu,⁸ S. Hamada,⁹ M. Hirai,¹⁰ and H. Miyatake⁵

¹*Instituto de Física, Universidade de São Paulo, P.O. Box 66318, 05389-970 São Paulo, SP, Brazil*

²*Center for Nuclear Study, University of Tokyo, RIKEN Campus, Hirosawa 2-1, Wako, Saitama 351-0198, Japan*

³*Department of Theoretical Physics, Research School of Physical Sciences and Engineering, Australian National University, Canberra ACT 0200, Australia*

⁴*Institute for Molecular Science, Okazaki 444, Japan*

⁵*Institute of Particle and Nuclear Studies, KEK, Tsukuba 305-0801, Japan*

⁶*Physics Department, Yamagata University, Yamagata 990-0021, Japan*

⁷*Cyclotron and Radioisotope Center, Tohoku University, Aoba, Miyagi 980-8578, Japan*

⁸*RIKEN, Wako, Saitama 351-0198, Japan*

⁹*JAERI, Tokai, Ibaraki 319-1106, Japan*

¹⁰*Department of Physics, University of Tokyo, Hongo, Bunkyo-ku, Tokyo 113-0033, Japan*

(Received 11 June 2002; published 3 June 2003)

The ground state and low-lying levels of the unbound ^{11}N nucleus were investigated with the three-neutron pickup reaction $^{14}\text{N}(^3\text{He}, ^6\text{He})^{11}\text{N}$. The energies and widths of these, experimentally observed, levels are compared with other measurements and calculations. Angular distributions were measured for the first time for this reaction. The distorted-wave Born approximation analysis confirms the spin assignments for the lowest levels.

DOI: 10.1103/PhysRevC.67.064601

PACS number(s): 25.55.Hp, 27.20.+n, 25.70.Ef, 25.60.Gc

I. INTRODUCTION

The $A=11$ system has been intensively studied because of the halo structure in ^{11}Li and the level inversion observed in ^{11}Be , where the lowest $\frac{1}{2}^+$ level lies lower in energy than the $\frac{1}{2}^-$ level expected as the ground state in the standard shell model. This level inversion has been partly explained as due to halo formation by the weakly bound valence neutron [1], although the association is still not clear. The valence particle in halo nuclei is usually in the s orbit; for the ^{11}Be ground state, most stripping reaction studies and model calculations have given an s -wave spectroscopic factor of 0.7 or larger [2], but one analysis of stripping data, which takes into account recoil excitation and breakup effects, has given a value as low as 0.19 (0.02) [3].

On the proton-rich side of the $A=11$ isobaric chain we have ^{11}N . ^{11}N is the mirror nucleus of the known halo nucleus ^{11}Be and all its levels are unbound for proton decay to ^{10}C . The investigation of the structure of this nucleus would be interesting in association with the isospin characteristic of the halo effect. This nucleus was first investigated by Benenson *et al.* [4] using the $^{14}\text{N}(^3\text{He}, ^6\text{He})^{11}\text{N}$ reaction. In this early work, only one clear peak was observed at 2.24 MeV above the $^{10}\text{C}+p$ threshold, and based on its measured width of 0.74(10) MeV, the level was assumed to be $\frac{1}{2}^-$. Due to the poor statistics of this experiment it was not possible to observe the $\frac{1}{2}^+$ level, which was predicted from the IMME (isobaric multiplet mass equation) to be 1.9 MeV above the proton decay threshold.

Later, other reactions were used to investigate the structure of ^{11}N . Axelsson *et al.* [5] and Markenroth *et al.* [6] used the resonant scattering $p(^{10}\text{C}, ^{11}\text{N})$ in inverse kinemat-

ics and Azhari *et al.* [7] measured the energy spectrum of the proton decay from ^{11}N . Oliveira *et al.* [8] and Lepine-Szilny *et al.* [9] used the heavy-ion transfer reactions and $^{10}\text{B}(^{14}\text{N}, ^{15}\text{B})^{11}\text{N}$ and $^{12}\text{C}(^{14}\text{N}, ^{15}\text{C})^{11}\text{N}$, respectively. The energies and widths of the levels observed for ^{11}N in these experiments are shown in Table II for comparison.

The observation of the $\frac{1}{2}^+$ ground state of ^{11}N was first reported by Axelsson *et al.* [5] at 1.30(4) MeV, with a width of 0.99(20) MeV. After this work some other results for the ^{11}N ground state have been reported. Oliveira *et al.* [8] gave the energy 1.63(5) MeV and a narrow width of 0.4(1) MeV. Azhari *et al.* [7] observed a barely separable shoulder on the low-energy side of the $\frac{1}{2}^-$ peak; if it is due to the $\frac{1}{2}^+$ ground state, it is at 1.45 (40) MeV with a lower limit on the width of 0.4 MeV. Markenroth *et al.* [6] observed the $\frac{1}{2}^+$ level at $1.27_{-0.05}^{+0.18}$ MeV and with a broad width of 1.44(20) MeV. As for the theoretical predictions, Fortune *et al.* [10] used a potential model to predict the $\frac{1}{2}^+$ ground state at 1.60(22) MeV with a width of $1.58_{-0.52}^{+0.75}$ MeV, while Barker [11] gave an energy and width with a potential model of 1.40 MeV and 1.01 MeV (or 1.60 MeV and 1.39 MeV from an alternative model). These and other theoretical values are also given in Table II.

Thus, both the experimental and theoretical values for the energy and width of the $\frac{1}{2}^+$ ground state of ^{11}N show considerable variations. It appears that not all of this is due to the use of different definitions for the energy and width of an unbound level [11] or due to the different reactions used to populate this level. The energy and width of this level are significant in the consideration of a possible halo structure in ^{11}N . Also, the energy and width of the ^{11}N ground state are very important in the interpretation of the two-proton decay

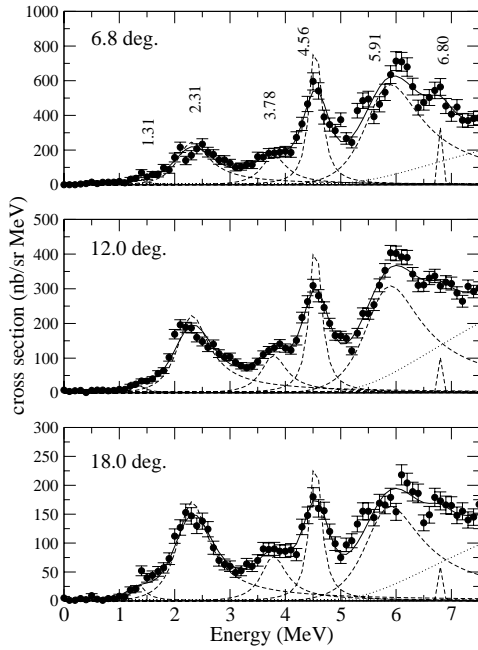


FIG. 1. ${}^6\text{He}$ energy spectra from the ${}^{14}\text{N}({}^3\text{He}, {}^6\text{He}){}^{11}\text{N}$ reaction at the laboratory angles indicated. Energies are measured from the ${}^{10}\text{C}+p$ threshold. The solid curves show the best fit to the measured data at eight angles, using Eq. (1), smeared over the experimental resolution of 200 keV. The dashed curves are the individual contributions (unsmeared) from each level included in the analysis. The dotted curves give the background contribution.

of the ${}^{12}\text{O}$ ground state [12], where depending on the energy of this level, the exotic diproton decay might be expected to compete with the sequential decay through the ${}^{11}\text{N}$ ground state.

The three-neutron (${}^3\text{He}, {}^6\text{He}$) pickup reaction has been shown to be a very useful spectroscopic tool to investigate the structure of proton-rich nuclei near the proton drip line. The angular distribution measured for this reaction has shown a strong dependence on the transferred angular momentum (L), and has allowed spin-parity assignments for several levels in ${}^{21}\text{Mg}$, ${}^{25}\text{Si}$, and ${}^{17}\text{Ne}$ in previous experiments [13–15]. Here we give information on the ground state and low-lying levels of the unbound ${}^{11}\text{N}$ nucleus obtained from the ${}^{14}\text{N}({}^3\text{He}, {}^6\text{He}){}^{11}\text{N}$ reaction.

This paper is divided into the following sections: the experimental setup and procedures are described in Sec. II, while the experimental results and R -matrix fits to the measured spectra are given in Sec. III. Section IV contains a distorted-wave Born approximation (DWBA) analysis of the angular distributions and a discussion on the spin assignments for the ${}^{11}\text{N}$ levels. Section V is devoted to a discussion on the energies and widths obtained for the ${}^{11}\text{N}$ levels and Sec. VI to a short discussion on the implications in the IMME. Finally, a summary is given in Sec. VII.

II. EXPERIMENT

The experiment was carried out with a sector-focusing cyclotron of the Center for Nuclear Study, University of

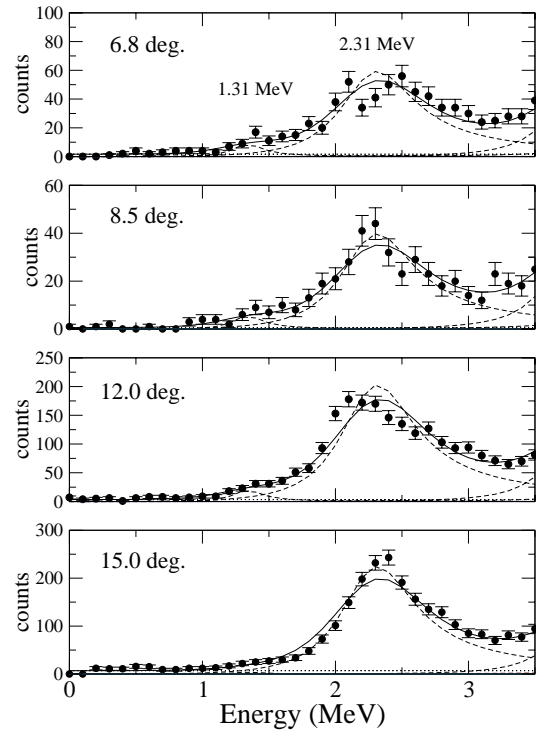


FIG. 2. ${}^6\text{He}$ energy spectra from the ${}^{14}\text{N}({}^3\text{He}, {}^6\text{He}){}^{11}\text{N}$ reaction at the laboratory angles indicated for the range of 0 to 3.5 MeV. Energies are measured from the ${}^{10}\text{C}+p$ threshold.

Tokyo, Japan. The incident energy of the ${}^3\text{He}$ beam was 73.40 ± 0.05 MeV and the average current obtained was about $0.5 \mu\text{A}$. The beam was transported into the scattering chamber, where a gas target with 99.95% isotopically enriched ${}^{14}\text{N}_2$ gas was placed. The gas cell was filled to a pressure of about 21 cm Hg during the measurements. A rectangular double-slit system was used to prevent particles from the windows (Havar foils) of the gas cell from entering the detectors. This double-slit system defined a solid angle in the order of 1 to 3 msr, depending on the detection angle. A ${}^{24}\text{Mg}$ metallic foil of $812 \pm 20 \mu\text{g}/\text{cm}^2$ thickness was also used as a target in a later run for energy calibration.

The momentum of the ${}^6\text{He}$ particles and other products from the reaction were analyzed by a quadrupole-dipole-dipole (QDD) spectrograph and detected by a hybrid-type gas proportional counter [16]. This proportional counter was specifically designed to minimize the background for this kind of experiment and was placed in the focal plane. A thin plastic scintillator was set just behind the proportional counter for energy and time-of-flight measurements. The particle identification was performed using a set of signals, namely, the energy signal from the plastic scintillator, energy loss from the proportional counter, and time of flight. The time of flight was obtained from the time interval between the cyclotron-rf and the fast signal from the plastic scintillator. The vertical position, perpendicular to the directions of momentum dispersion as well as the particle trajectory, was also measured on the focal plane and used to reduce the background not arising from the target. Pileup rejection was

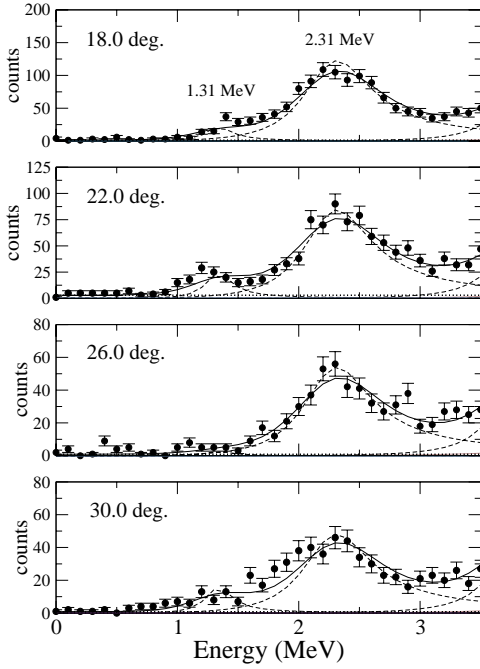


FIG. 3. ^6He energy spectra from the $^{14}\text{N}(^3\text{He}, ^6\text{He})^{11}\text{N}$ reaction at the laboratory angles indicated for the range of 0 to 3.5 MeV. Energies are measured from the $^{10}\text{C}+p$ threshold.

also applied to reduce even more the background since the cross section for this ($^3\text{He}, ^6\text{He}$) reaction is very small.

III. ENERGY SPECTRA ANALYSIS

The momentum spectra for the outgoing ^6He nuclei were obtained at eight angles ($\theta_{\text{LAB}}=6.8^\circ, 8.5^\circ, 12.0^\circ, 18.0^\circ, 22.0^\circ, 26.0^\circ, \text{ and } 30.0^\circ$). The momentum spectrum measured at $\theta_{\text{LAB}}=12.0^\circ$ was converted to an energy spectrum using the calibration obtained with the known states of ^{21}Mg from the $^{24}\text{Mg}(^3\text{He}, ^6\text{He})^{21}\text{Mg}$ reaction [13], which was measured with the ^{24}Mg solid target in the same experimental run. The momentum spectra at other angles were then converted to energy spectra. Energy spectra obtained at $\theta_{\text{LAB}}=6.8^\circ, 12.0^\circ, \text{ and } 18.0^\circ$ are shown in Fig. 1, normalized for integrated charge, effective target thickness of gas cell, and solid angles. The uncertainties are statistical errors. The energy in these spectra corresponds to the energy above the $^{10}\text{C}+p$ threshold (decay energy), for which the Q value is -22.788 MeV. The binning was set to 100 keV. The overall energy resolution of about 200 keV full width at half maximum (FWHM) is due mainly to the different energy losses of the ^3He beam and ^6He particles in the gas target system.

In the $^{14}\text{N}(^3\text{He}, ^6\text{He})^{11}\text{N}$ reaction, the populated levels in ^{11}N are observed as peaks in the ^6He spectrum; because all levels of ^{11}N are unstable against breakup into $^{10}\text{C}+p$, these peaks sit on a background due at least in part to alternative reaction processes. Also, for energies above about 4 MeV, other breakup channels, such as $^9\text{B}+2p$ decay, are open.

The experimental energy spectra, shown in Figs. 1–4, present some well defined and intensely populated peaks at

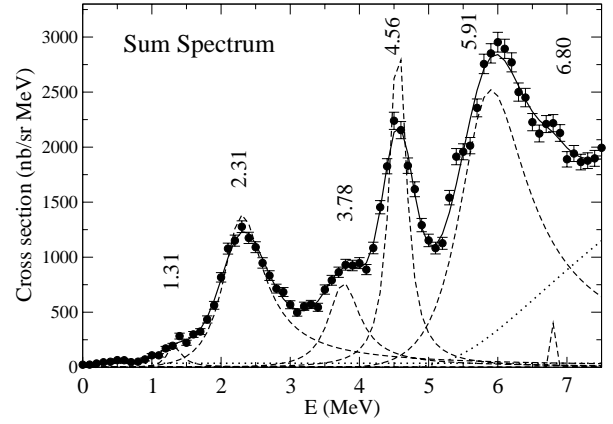


FIG. 4. Summed energy spectrum for the $^{14}\text{N}(^3\text{He}, ^6\text{He})^{11}\text{N}$ reaction. As in Fig. 1, except that the curves are from a best fit to this summed spectrum.

2.31, 4.56, and 5.91 MeV. At 3.78 MeV, incrustated between the larger peaks at 2.31 and 4.56 MeV, a “bump” is visible, which corresponds to the $3/2^+$ resonance, observed in previous works [5,6,8,9] around 3.61–3.75 MeV. On the low energy tail of the much more strongly populated 2.31-MeV peak a shoulder is visible around 1.31 MeV. The ground state resonance of ^{11}N is expected in this energy region, previous works have observed it around 1.27 to 1.63 MeV [5,6,8].

We therefore attempt to fit the observed spectra with a function of the form

$$N(E, \theta) = \sum_i b_i(\theta) N_i(E) + c(\theta) + d(\theta) P_b(E), \quad (1)$$

where

$$N_i(E) = \frac{\Gamma_i(E)}{[E_{ri} + \Delta_i(E) - E]^2 + 1/4\Gamma_i^2(E)}. \quad (2)$$

The sum is over the levels of ^{11}N , each of which is described by the one-level one channel approximation of R -matrix theory [17]. The decay width is given by $\Gamma_i(E) = 2\gamma_i^2 P_i(E)$ and $\Delta_i(E) = -\gamma_i^2 [S_i(E) - S_i(E_{ri})]$. $P_i(E)$ and $S_i(E)$ are the energy-dependent penetration and shift factors for the $^{10}\text{C}+p$ channel. The background is assumed to be partly flat (to allow for possible random coincidences) and partly proportional to an s -wave penetration factor for the $^9\text{B}+2p$ channel, $P_b(E)$. For each channel, we use the conventional value of the channel radius $a = 1.45(A_1^{1/3} + A_2^{1/3})$ fm [17]. Then, for each ^{11}N level i , the adjustable parameters are resonance energy E_{ri} , reduced width γ_i^2 , and strength $b_i(\theta)$. $b_i(\theta)$, $c(\theta)$, and $d(\theta)$ are independently adjustable at each angle.

In order to fit the data for $E \leq 7.5$ MeV, we include contributions from six levels in ^{11}N . The factors $P_i(E)$ and $S_i(E)$ in Eq. (1) depend on the relative angular momentum ℓ_i for their decay into the $^{10}\text{C}+p$ channel, and thus, on the total angular momentum assigned for each level in ^{11}N . Here, we have assumed $J_i^\pi = \frac{1}{2}^+, \frac{1}{2}^-, \frac{5}{2}^+, \frac{3}{2}^-, \frac{5}{2}^-, \text{ and } \frac{3}{2}^-$

TABLE I. Values of ^{11}N level parameters from the best fit to summed spectrum. Energies are measured from the $^{10}\text{C}+p$ threshold. All the energies and widths are in MeV.

Level	J^π	l_i	E_{ri}	γ_i^2	b_i	Γ_i^0	A_i
1	$\frac{1}{2}^+$	0	$1.323_{-0.046}^{+0.058}$	$0.29_{-0.28}^{+0.43}$	26	$0.24_{-0.23}^{+0.29}$	77
2	$\frac{1}{2}^-$	1	$2.355_{-0.015}^{+0.015}$	$0.90_{-0.09}^{+0.10}$	631	$0.76_{-0.06}^{+0.07}$	1630
3	$\frac{5}{2}^+$	2	$3.794_{-0.038}^{+0.059}$	$0.88_{-0.29}^{+0.39}$	261	$0.56_{-0.16}^{+0.19}$	676
4	$\frac{3}{2}^-$	1	$4.559_{-0.012}^{+0.011}$	$0.117_{-0.019}^{+0.023}$	437	$0.28_{-0.05}^{+0.06}$	1359
5	$\frac{5}{2}^-$	1	$6.030_{-0.034}^{+0.042}$	$1.51_{-0.15}^{+0.19}$	2288	$1.45_{-0.12}^{+0.13}$	5521
6	$\frac{3}{2}^-$	1	$6.81_{-0.41}^{+0.20}$	$0.002_{-0.002}^{+0.094}$	4	$0.01_{-0.01}^{+0.34}$	13

for the six lowest levels in ^{11}N . These assignments are based largely on the levels shown in Fig. 1 of Ref. [18] (for the mirror nucleus ^{11}Be). For the $^{14}\text{N}(^3\text{He}, ^6\text{He})^{11}\text{N}$ reaction, three-neutron pickup can populate directly Cohen-Kurath (CK) states (states in a p -shell basis), so that in the region studied, one might expect the $\frac{1}{2}^-$, $\frac{3}{2}^-$, $\frac{5}{2}^-$, and $\frac{3}{2}^-$ states to be formed strongly. Population of positive-parity states based on a ^{10}C core would require a two-step process, and thus one would expect the low-lying $\frac{1}{2}^+$ and $\frac{5}{2}^+$ states to be formed more weakly. These assignments for the four lowest levels in ^{11}N have been adopted previously [5–9]. The $\frac{5}{2}^-$ fifth level would require $\ell=3$ protons to decay to the ground state of

^{10}C , and these are not present in a CK state, so it is assumed that this level decays to $^{10}\text{C}(2^+)+p$ with $\ell=1$ protons [7]. For the other five levels, we assume decay to $^{10}\text{C}(0^+)+p$ with $\ell_i=0, 1, 2, 1,$ and 1 , respectively.

In a simultaneous fit of the data for all eight angles, there are 608 data points and 76 adjustable parameters. In principle, there could be interference between the contributions from the different levels; this has been neglected in Eq. (1) for simplicity, as the additional parameters required with interference could not be well determined with the available data.

For comparison with the data, the function $N(E, \theta)$ given by Eq. (1) is smeared over the experimental energy resolution of 200 keV. The best fit to all the data has $\chi^2=748$. This fit is shown in Fig. 1 for three of the angles. Figures 2 and 3 show the spectra between 0 and 3.5 MeV for all eight angles measured on an expanded scale. In order to improve the statistics and to better determine the parameters of the levels, a summed spectrum was obtained by adding the normalized energy spectra from each angle, with the uncertainty at each energy in the sum spectrum equal to the square root of the sum of the squares of the uncertainties in each individual angle spectrum. The best fit to the sum spectrum is shown in Fig. 4; it has $\chi_{\text{min}}^2=100.2$, for 76 data points and 20 adjustable parameters, giving a reduced $\chi_{\nu}^2=1.79$. The values of the parameters E_{ri} , γ_i^2 , and b_i are given in Table I, together with derived values of the observed width Γ_i^0 defined by

$$\Gamma_i^0 = \Gamma_i / [1 + \gamma_i^2 (dS_i/dE)_{E_{ri}}] \quad (3)$$

TABLE II. Decay energy above the $^{10}\text{C}+p$ threshold and widths of the ^{11}N resonances measured in this work and from the references indicated. All the energies and widths are in MeV.

J^π	This work		Oliveira <i>et al.</i> [8] ^a		Experimental papers		Markenroth <i>et al.</i> [6] ^c		Axelsson <i>et al.</i> [5] ^d	
	E_m	Γ_m	E_{decay}	Γ	E_{decay}	Γ	E_{decay}	Γ	E_{decay}	Γ
$\frac{1}{2}^+$	1.31(5)	0.24(24)	1.63(5)	0.4(1)			$1.27_{-0.05}^{+0.18}$	1.44(20)	1.30(4)	0.99(20)
$\frac{1}{2}^-$	2.31(2)	0.73(6)	2.16(5)	0.25(8)	2.18(5)	0.44(8)	2.01(15)	0.84(20)	2.04	0.69
			3.06(8)	$\leq 0.10(8)$	(2.92)	(0.1)				
$\frac{5}{2}^+$	3.78(5)	0.56(17)	3.61(5)	0.50(8)	3.63(5)	0.40(8)	3.75(5)	0.60(5)	3.72	0.60
$\frac{3}{2}^-$	4.56(1)	0.30(5)	4.33(5)	0.45(8)	4.39(5)	$\leq 0.2(1)$	4.33(5)	0.27	4.32	0.07
$(\frac{5}{2}^-)$	5.91(3)	1.30(9)	5.98(10)	0.10(6)	5.87(15)	0.7(2)			5.50	1.5
$(\frac{3}{2}^-)$	6.80(30)		6.54(10)	0.10(6)						
J^π	Fortune [10]		Barker [11]		Theoretical papers		Grévy [22]			
	E_{decay}	Γ	E_{decay}	Γ	E_{decay}	Γ	E_{decay}	Γ		
$\frac{1}{2}^+$	1.60	1.58	1.4	1.01	1.1	0.9	1.2	1.2		
$\frac{1}{2}^-$	2.49	1.45	2.21	0.91	1.6	0.3	2.1	1.0		
$\frac{5}{2}^+$	3.90	0.88	3.88	0.72	3.8	0.6	3.7	1.0		

^aUsing heavy-ion transfer reaction $^{10}\text{B}(^{14}\text{N}, ^{13}\text{B})^{11}\text{N}$ at GANIL.

^bUsing heavy-ion transfer reaction $^{12}\text{C}(^{14}\text{N}, ^{15}\text{C})^{11}\text{N}$ at GANIL.

^cUsing resonant scattering $p(^{10}\text{C}, ^{11}\text{N})$ reaction at GANIL and MSU.

^dUsing resonant scattering $p(^{10}\text{C}, ^{11}\text{N})$ reaction at GANIL.

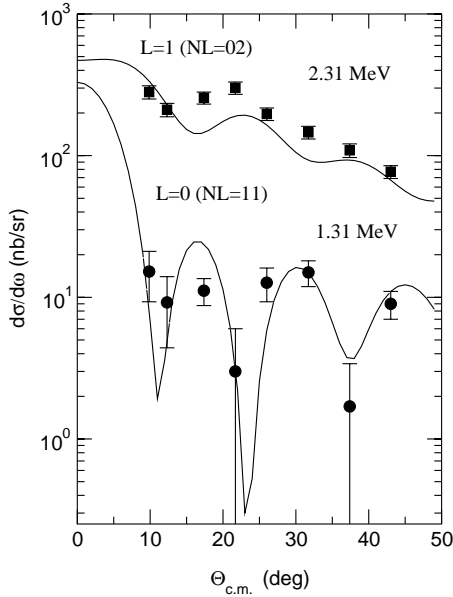


FIG. 5. Angular distributions for the $^{14}\text{N}(^3\text{He},^6\text{He})^{11}\text{N}$ reaction for the transitions denoted. The curves are the results of DWBA calculations with the transferred angular momenta (L) indicated.

with $\Gamma_i = 2\gamma_i^2 P_i(E_{ri})$, and of the peak area A_i defined by

$$A_i = \pi b_i / [1 + \gamma_i^2 (dS_i/dE)_{E_{ri}}]. \quad (4)$$

The uncertainties in these parameters correspond to increases in χ^2 to $\chi_{min}^2 + \chi_v^2$. For comparison with values obtained by other experiments and theoretical predictions we give in Table II the corresponding values of the peak energy E_m (energy for the maximum contribution of the level to the calculated spectrum) and the corresponding FWHM, Γ_m , where average uncertainties are given.

Because the ground state is sitting on the tail of the 2.31-MeV peak, which is populated much more strongly, and because of the energy resolution, one does not see a ground-state “peak” in the experimental data, but at most a plateau or shoulder, as is shown in the solid curves in Figs. 2–4. To investigate if the evidence for the ground state is statistically significant, we have fitted the summed spectrum for $E = 0$ –5 MeV with and without a contribution from the ground state (and with fixed values of the parameters for the levels 5 and 6, and of the background parameter d). The best fit with the ground state included has $\chi^2 = 51.6$, while the best fit with no contribution from the ground state has $\chi^2 = 124.4$. The contributions to χ^2 from the region $E = 1$ –2 MeV for these two cases are 11.6 and 78.0, respectively. This shows that the ground state is contributing significantly to the present data. Also, this peak/shoulder has 350 ± 48 counts summing all angle spectra, and thus, a statistical significance of 7σ .

IV. ANGULAR DISTRIBUTION ANALYSIS

From the simultaneous fit to all the spectra, values are obtained for the differential cross section for the $^{14}\text{N}(^3\text{He},^6\text{He})^{11}\text{N}$ reaction at eight angles for each level in

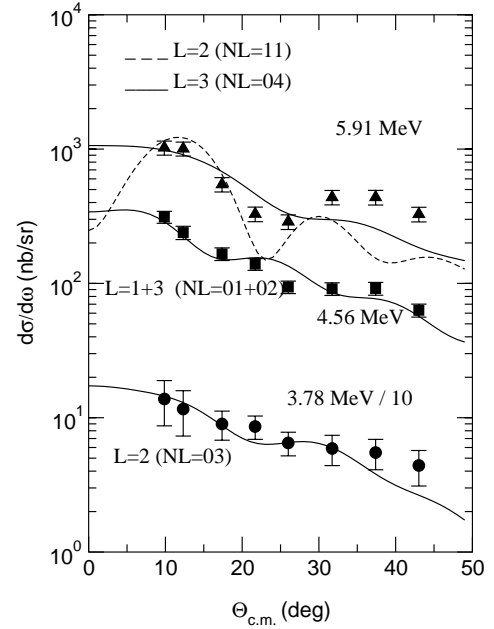


FIG. 6. Angular distributions for the $^{14}\text{N}(^3\text{He},^6\text{He})^{11}\text{N}$ reaction for the transitions denoted. The curves are the results of DWBA calculations with the transferred angular momenta (L) indicated. The N and L in parentheses are choices for the number of radial nodes and the orbital angular momentum of the $3n$ cluster relative to the core of the residual nucleus adopted in the calculation.

^{11}N , and these are shown in Figs. 5 and 6 for the first five levels. The measured differential cross sections are, in general, very small, being in a range of a few tens of nb/sr for the ground state and a few hundreds of nb/sr for the other levels; the sixth level is too weakly populated by this reaction for its angular distribution to be significant. The uncertainties on the experimental differential cross sections were obtained by taking into account the following uncertainties: the statistical uncertainties in the yield and in the background under the peaks, the uncertainties in the target thickness and solid angle, and an estimated uncertainty of 10–15% due to the deconvolution of the peaks. The final values of the uncertainties were estimated to be between 12% and 30%, except for the ground state where the uncertainties are in the range of 40–50%.

The analysis of the characteristic behavior at the forward angles in the experimental angular distributions has been made in terms of the exact finite-range DWBA, using the computer code TWOFNR [19]. The optical potential parameters used in the DWBA calculations were basically the same as used before in the analysis of angular distributions for the $^{24}\text{Mg}(^3\text{He},^6\text{He})^{21}\text{Mg}$ reaction [13] and for the $^{20}\text{Ne}(^3\text{He},^6\text{He})^{17}\text{Ne}$ reaction [15] and they are listed in Table III. A change in the real radius of the outgoing channel from the set of parameters used in the previous experiment has been considered in order to better reproduce the oscillations, although no clear attempt to fit the data has been made by changing any other optical potential. For the bound state parameters of the $3n$ cluster in ^{14}N and ^6He the conventional $r_0 = 1.25$ fm and $a = 0.65$ fm were adopted. The radius was defined as $R = r_0 A^{1/3}$, and the potential depths were adjusted

TABLE III. Optical and binding potential parameters. The radii are given by $R_x = r_x \times M_T^{1/3}$.

Set	V (MeV)	r_R (fm)	a_R (fm)	W_V^a (MeV)	r_I (fm)	a_I (fm)	r_C (fm)
${}^3\text{He} + {}^{14}\text{N}$	160.00	1.633	0.375	35.00	1.015	1.767	1.3
${}^6\text{He} + {}^{11}\text{N}$	64.70	1.350	0.717	13.00	1.500	0.800	1.3
$3n + {}^{11}\text{N}$	b	1.25	0.65				
$3n + {}^3\text{He}$	b	1.25	0.65				

^aThe imaginary potential is a volume type Woods-Saxon potential for both systems.

^bThe depth was adjusted to reproduce the binding energy.

to reproduce the binding energies.

In the case of the ${}^{14}\text{N}({}^3\text{He}, {}^6\text{He}){}^{11}\text{N}$ reaction, the spin of the ${}^{14}\text{N}$ target nucleus is 1^+ and for ${}^3\text{He}$ it is $\frac{1}{2}^+$ and thus, more than one transferred angular momentum L can contribute to produce the angular momentum J of the final state in the residual ${}^{11}\text{N}$ nuclei. For instance, to produce the final $J^\pi = \frac{1}{2}^+$ state, the reaction can proceed by transferring angular momentum $L=0$ and/or $L=2$, to give $J^\pi = \frac{3}{2}^-$ by $L=1$ and/or $L=3$, and $J^\pi = \frac{5}{2}^+$ by $L=2$ and/or $L=4$. However, for $J^\pi = \frac{1}{2}^-$ only $L=1$ is possible. The parity of any transition is given by $\pi = (-1)^L$.

Any transitions should also satisfy the energy conservation rule [20],

$$\sum (2n_i + l_i) = 2N_j + L_j + 2\nu + \lambda, \quad (5)$$

where n_i and l_i are the number of radial nodes (excluding the origin) and the orbital angular momentum of each constituent nucleon in the shell model; N_j and L_j ($j=1,2$) are the number of radial nodes and the orbital angular momentum of the $3n$ cluster relative to the core of the outgoing nucleus and the residual nucleus, respectively. The numbers ν and λ stand for the number of radial nodes and angular momentum of the internal motion in the $3n$ cluster. Since a direct one-step process of a $3n$ -cluster transfer was assumed for the (${}^3\text{He}, {}^6\text{He}$) reaction, the quantum numbers for the internal motion of all three identical fermions are $\nu=0$ and $\lambda=1$ for the transitions to the low-lying states. This implies that the $3n$ cluster in ${}^6\text{He}$ should have $J_x^\pi = \frac{3}{2}^-$ and $L_2=1$, $N_2=0$ for the motion with respect to the ${}^3\text{He}$ core. Thus, for the low-lying states of the residual nucleus, the $3n$ -cluster in ${}^{14}\text{N}$ should have $L_1=1$, $N_1=1$ for the motion with respect to the ${}^{11}\text{N}$ core for $L=0$ transitions, where $\vec{L} = \vec{L}_1 + \vec{L}_2$. For transitions with $L=2$, we have $2N_1 + L_1 = 3$ for ${}^{11}\text{N}$, which gives two possibilities for the quantum numbers of the relative motion: $L_1=3$, $N_1=0$ or $L_1=1$, $N_1=1$. These two possibilities for the quantum numbers did not change significantly the positions of the maxima and minima in the calculated angular distributions, but, since they give small changes in the relative intensity of the maxima, the set that better reproduced the experimental angular distributions was chosen, and they are indicated in Figs. 5 and 6.

The results of the DWBA calculations for the angular distributions are presented in Figs. 5 and 6. Since few angles have been measured and due to the complexity of this reaction and of the approximations assumed in the calculations, such as the cluster transfer of three neutrons, only a qualitative analysis of the angular distributions is possible. A normalization of the calculated angular distributions to the data has been applied. The angular distributions calculated by the DWBA show strong oscillation and distinct patterns at forward angles for different L . The general shapes of the angular distributions at forward angles and the oscillations phases (maximum and minimum angles) were reasonably well reproduced by the calculations. As can be seen in Figs. 5 and 6, there is a smooth shift of the first minimum angle as a function of L ($\Theta_{\text{CM}} = 11^\circ$ for $L=0$, $\Theta_{\text{CM}} = 16^\circ$ for $L=1$, and so on), which supports the general feature of L dependence, as expected in direct multinucleon transfer reactions [20].

For the transition to the 1.31-MeV ground state, shown in Fig. 5, the angular distribution seems to be reasonably reproduced by a DWBA calculation with $L=0$ only. This level would correspond to an sd -shell proton coupled to ${}^{10}\text{C}$, i.e., ${}^{10}\text{C}(0^+) \otimes \pi 2s_{1/2}$ and/or ${}^{10}\text{C}(2^+) \otimes \pi d_{5/2}$ configurations. Unfortunately, since we can not get a quantitative contribution from the two possible angular momenta transferred, it is not possible to clearly distinguish between these two possible configurations with the present angular distribution analysis.

For the 2.31-MeV transition, which is the well known $\frac{1}{2}^-$ resonance, the angular distribution seems to be due to $L=1$ angular momentum transferred, as expected. The other level in ${}^{11}\text{N}$ which has a firm spin assignment is the $\frac{5}{2}^+$ level at 3.78 MeV. This $d_{5/2}$ resonance has been strongly populated in the two heavy-ion transfer reaction, ${}^{12}\text{C}({}^{14}\text{N}, {}^{15}\text{C}){}^{11}\text{N}$ [8] and ${}^{10}\text{B}({}^{14}\text{N}, {}^{15}\text{B}){}^{11}\text{N}$ [9], but is not as strongly populated by the (${}^3\text{He}, {}^6\text{He}$) reaction. This $\frac{5}{2}^+$ level also would correspond to an sd -shell proton coupled to ${}^{10}\text{C}$, i.e., ${}^{10}\text{C}(0^+) \otimes \pi d_{5/2}$ and/or ${}^{10}\text{C}(2^+) \otimes \pi 2s_{1/2}$ configurations.

Thus, our data confirm the spin assignment for the three lowest levels in ${}^{11}\text{N}$. In particular, our data confirm the assignment $J^\pi = \frac{1}{2}^+$ and $J^\pi = \frac{1}{2}^-$ for the first two transitions, which shows the same spin inversion for the ground-state spin as observed for ${}^{11}\text{Be}$.

The 4.56-MeV level and, in particular, the level at 5.91 MeV are strongly populated by this three-neutron pickup reaction. The angular distribution for the 4.56-MeV level seems to be well reproduced by a combination of $L=1+3$ angular distribution, which would favor a negative parity assignment, see Fig. 6. This L assignment and the narrow width observed for this level in this and in the other experiments [7–9] would indicate that it is the analog of the $J^\pi = \frac{3}{2}^-$ state at 2.69 MeV in ${}^{11}\text{Be}$ [23]. The level at 5.91 MeV has been tentatively assigned by the other experiments as $J^\pi = \frac{5}{2}^-$, based on shell model calculations for ${}^{11}\text{N}$ [7]. The angular distribution for this level seems to be reproduced by an $L=3$ angular momentum transferred, although $L=2$ is also possible (dashed line in Fig. 6). $L=3$ is consistent with the $\frac{5}{2}^-$ assignment.

V. DISCUSSION ON THE ENERGIES AND WIDTHS

The energies and widths E_m and Γ_m obtained in this work for the six lowest levels in ^{11}N and their uncertainties are presented in Table II, where they are compared with the values obtained by other experimental works and theoretical predictions. Our data seem to be in good agreement with the results of most experiments and theoretical predictions, although some important differences are apparent. The $\frac{1}{2}^+$ ground state is observed at 1.31(5) in this work. This value agrees with the energy obtained by Markenroth *et al.* [6] and Axelsson *et al.* [5] but is lower when compared with the results by Oliveira *et al.* [8]. The width for this level is obtained in the range of $\Gamma=0$ to 500 keV, and it is in better agreement with the value obtained in another transfer reaction experiment by Oliveira *et al.*, which gives $\Gamma=400(100)$ keV. As pointed out by Barker [11], there may be some difference in the definitions of energy and width for unbound levels used in these experimental works; and although all the definitions are expected to give practically the same value for narrow levels, they can differ for broad levels. However, even by taking into account possible differences in the energy and width definition for the $\frac{1}{2}^+$ level, the difference from the resonance scattering and transfer reactions works seems to be too large. The width for this state is directly related to the single particle nature of this state. Assuming $\Gamma_{sp}=1.28$ MeV, from Sherr and Fortune [24], we obtain a spectroscopic factor in the range of 0.1 to 0.2. This low spectroscopic factor would be consistent with a large d -wave admixture in the configuration of the $J^\pi=\frac{1}{2}^+$ level. A similar value for the spectroscopic factor is obtained in the analysis of Oliveira *et al.* [8] for the ^{11}N ground state and also for the ^{11}Be ground state in the recent analysis of the $^{11}\text{Be}(p,d)^{10}\text{Be}$ reaction by Johnson *et al.* [3].

The $\frac{1}{2}^-$ level in ^{11}N is strongly populated in most reactions. The energy and width $E=2.31(2)$ MeV and $\Gamma=0.73(6)$ MeV obtained in this work agree very well within the experimental error with the values obtained in the earlier experiment using the same $^{14}\text{N}(^3\text{He}, ^6\text{He})^{11}\text{N}$ reaction by Benenson *et al.*, $E=2.24(10)$ MeV and $\Gamma=0.74(10)$. The energy for this state is, however, about 200 keV higher here when compared with the other works.

The energies and widths for the $\frac{5}{2}^+$ level at 3.78 MeV and for the $\frac{3}{2}^-$ levels at 4.56 MeV obtained in this work are also in good agreement with the values obtained in the other works. The fifth level at 5.91 MeV is strongly populated by this pickup reaction. It has been assumed that this level decays to $^{10}\text{C}(3.35)+p$ channel giving a relative angular momentum $\ell=1$ for the proton, which gives a reduced width $\gamma^2=1.912$ MeV.

VI. ISOBARIC MULTIPLY MASS EQUATION

The decay energy of 1.31(5) MeV for the $\frac{1}{2}^+$ ground state in ^{11}N would correspond to a mass excess of ME = 24.30(5) and for the 2.31(2) MeV $\frac{1}{2}^-$ state a ME = 25.30(2) MeV is obtained. This value for the mass excess of ^{11}N ground state would allow the sequential proton decay of ^{12}O through this state.

The IMME relates the mass excess of the four members of an isobaric multiplet by the following expression:

$$M(A, T_z) = a + b \times T_z + c \times T_z^2 + d \times T_z^3, \quad (6)$$

where T_z is the isospin projection and a, b, c , and d are the coefficients.

The most important coefficient to test the IMME equation is the d coefficient. If the charge-dependent interaction is two body and treated as a first order perturbation and if the isospin mixing is neglected, then the d coefficient should be zero. In terms of the mass excess of the quartets it is given by

$$d = \frac{1}{6} \times (M_{^{11}\text{Be}} - M_{^{11}\text{N}}) - \frac{1}{2} \times (M_{^{11}\text{C}} - M_{^{11}\text{B}}). \quad (7)$$

A compilation of d coefficients for twenty-two isobaric quartets from $A=7$ to $A=41$ has been made by Antony *et al.* [25]. It was found that they are consistent with zero, the upper limit of their absolute values being around 7 keV, except for the $A=9$ which has a nonzero coefficient (5.2 ± 1.7) keV. The d coefficient determined here for the $\frac{1}{2}^-$ state is consistent with zero. However, for the $\frac{1}{2}^+$ state the value obtained is $d=102(30)$ keV. As pointed out by Sherr and Fortune [24], such a d value would correspond to too large an isospin mixing, indicating a possible misidentification of the $T=\frac{3}{2}$ states in ^{11}C and/or ^{11}B .

Another possibility for the presence of d coefficient in the IMME is the expansion of the wave function due to the Coulomb effects as the neutrons in the neutron-rich members are converted to protons. This expansion, due to the Coulomb repulsion, can be more pronounced for barely bound particles in the $s_{1/2}$ orbit. Although this effect has been estimated to be small for the $A=9$ quartet [26] (in the order of few keV), it has not been evaluated for a quartet where the proton-rich member is unbound. A large d coefficient can also be originated due to a large differential energy shift between the s and p orbits and one of the mechanism for this shift is the Thomas-Ehrman effect [27]. To explain the large shift for the ^{11}Be - ^{11}N mirror pair, Aoyama [28] has proposed that Coulomb barrier top effect could produce a higher order Thomas-Ehrman shift due to the difference between the mirror core+ N wave functions.

The large d coefficient of the IMME analysis for the $A=11$ system is an open question and can be an interesting problem to be investigated.

VII. SUMMARY

The angular distributions have been measured for the first time for this $^{14}\text{N}(^3\text{He}, ^6\text{He})^{11}\text{N}$ reaction. The angular distributions for the low-lying states in ^{11}N have shown distinct behaviors, indicating that they may have different transferred

angular momenta. The $\frac{1}{2}^+$ ground state of ^{11}N gives a weak but statistically significant contribution to the present data. An analysis with DWBA calculations confirms the assignment of $J^\pi = \frac{1}{2}^+$ and $J^\pi = \frac{1}{2}^-$ for the ground state and the first excited state. Thus, in ^{11}N , the anomalous situation that the $\frac{1}{2}^+$ state comes lower than the $\frac{1}{2}^-$ is the same as observed in ^{11}Be . The narrow width found in this work for the $\frac{1}{2}^+$ ground state favors a small spectroscopic factor.

ACKNOWLEDGMENTS

The authors are grateful to the cyclotron crew of the Center for Nuclear Study and to Alinka Lépine-Szily for valuable discussion. The first author (V.G.) was financially supported by the Inoue Foundation of Japan and by FAPESP (Fundação de Amparo a Pesquisa do Estado de São Paulo) during this work.

-
- [1] A. Ozawa *et al.*, Phys. Lett. B **334**, 18 (1994).
 - [2] T. Aumann *et al.*, Phys. Rev. Lett. **84**, 35 (2000).
 - [3] R.C. Johnson *et al.*, in *Experimental Nuclear Physics in Europe*, edited by Berta Rubio, Manuel Lozano, and William Gelletly, AIP Conf. Proc. No. 495 (AIP, Melville, NY, 1999), p. 297.
 - [4] W. Benenson *et al.*, Phys. Rev. C **9**, 2130 (1974).
 - [5] L. Axelsson *et al.*, Phys. Rev. C **54**, R1511 (1996).
 - [6] K. Markenroth *et al.*, Phys. Rev. C **62**, 034308 (2000).
 - [7] A. Azhari *et al.*, Phys. Rev. C **57**, 628 (1998).
 - [8] J.M. Oliveira, Jr., *et al.*, Phys. Rev. Lett. **84**, 4056 (2000).
 - [9] A. Lépine-Szily *et al.*, Phys. Rev. Lett. **80**, 1601 (1998).
 - [10] H.T. Fortune, D. Koltenuk, and C.K. Lau, Phys. Rev. C **51**, 3023 (1995).
 - [11] F.C. Barker, Phys. Rev. C **53**, 1449 (1996).
 - [12] R.A. Kryger *et al.*, Phys. Rev. Lett. **74**, 860 (1995).
 - [13] S. Kubono *et al.*, Nucl. Phys. **A537**, 153 (1992).
 - [14] S. Kubono *et al.*, Nucl. Phys. **A621**, 195c (1997).
 - [15] V. Guimarães *et al.*, Phys. Rev. C **58**, 116 (1998).
 - [16] M.H. Tanaka, S. Kubono, and S. Kato, Nucl. Instrum. Methods Phys. Res. **195**, 509 (1982).
 - [17] A.M. Lane and R.G. Thomas, Rev. Mod. Phys. **30**, 257 (1958).
 - [18] G.B. Liu and H.T. Fortune, Phys. Rev. C **42**, 167 (1990).
 - [19] M. Igarashi (unpublished).
 - [20] A. Arima and S. Kubono, in *Treatise on Heavy-Ion Science*, edited by D. A. Bromley (Plenum, New York, 1984), Vol. 1, Chap. 6.
 - [21] P. Descouvemont, Nucl. Phys. **A615**, 261 (1997).
 - [22] S. Grévy *et al.*, Phys. Rev. C **56**, 2885 (1997).
 - [23] F. Cappuzzello *et al.*, Phys. Lett. B **516**, 21 (2001).
 - [24] R. Sherr and H.T. Fortune, Phys. Rev. C **64**, 064307 (2001).
 - [25] M.S. Antony *et al.*, ADND **33**, 461 (1985).
 - [26] G. Bertsch and S. Kahana, Phys. Lett. **33B**, 193 (1970).
 - [27] J.B. Ehrman, Phys. Rev. **81**, 412 (1951); R.G. Thomas, *ibid.* **88**, 1109 (1952).
 - [28] S. Aoyama, Phys. Rev. C **62**, 034305 (2000).